

Article

Phase Change Material Composite Battery Module for Thermal Protection of Electric Vehicles: An Experimental Observation

Alexander C. Budiman ^{1,*}, Brian Azzopardi ^{2,3}, Sudirja ¹, Muhammad A. P. Perdana ¹, Sunarto Kaleg ¹, Febriani S. Hadiastuti ⁴, Bagus A. Hasyim ⁴, Amin ¹, Rina Ristiana ¹, Aam Muharam ¹ and Abdul Hapid ¹

¹ Research Center for Transportation Technology, National Research and Innovation Agency (BRIN), KST Samaun Samadikun BRIN Jl. Sangkuriang, Bandung 40135, Indonesia

² MCAST Energy Research Group, Institute of Engineering and Transport, Malta College of Arts, Science and Technology (MCAST), PLA 9032 Paola, Malta; brian.azzopardi@mcast.edu.mt

³ The Foundation for Innovation and Research—Malta, BKR 4012 Birkirkara, Malta

⁴ Departement of Mechanical Engineering, Institut Teknologi Sepuluh September, Surabaya 60111, Indonesia

* Correspondence: alex003@brin.go.id

Abstract: A composite container for an electric vehicle (EV) battery module filled with a phase-change material (PCM) was experimentally tested at various discharge rates. The average cell temperatures at 1 C, 2 C, and 4 C discharge rates, respectively, might reach 38 °C, 50 °C, and 70 °C in the absence of any heat-absorbing material. The temperature was noticeably lower with PCM present than with a conventional battery module. For instance, at 4 C discharge rates, none of the battery cells inside the PCM-filled module were able to reach 70 °C. Unfortunately, the PCM addition also degraded the composite's tensile qualities. Further investigations used Paraffin-20 and Caprylone since PCMs provide a notably different thermal performance due to their distinctive latent heat profiles. It was observed that a high melting temperature of the paraffin mixture, despite its slightly lower latent heat capacity compared to Caprylone, could lead to a more uniform temperature. Overall, both PCMs can be used as passive protection against any potential thermal abuses in EV battery modules, while in terms of mechanical strength, the use of a composite reinforcement material is strongly encouraged.

Keywords: battery thermal management system; composites; electric vehicles; heat storage; latent heat; temperature uniformity



Citation: Budiman, A.C.; Azzopardi, B.; Sudirja; Perdana, M.A.P.; Kaleg, S.; Hadiastuti, F.S.; Hasyim, B.A.; Amin; Ristiana, R.; Muharam, A.; et al. Phase Change Material Composite Battery Module for Thermal Protection of Electric Vehicles: An Experimental Observation. *Energies* **2023**, *16*, 3896. <https://doi.org/10.3390/en16093896>

Academic Editors: Jong Hoon Kim and Hugo Morais

Received: 24 March 2023

Revised: 24 April 2023

Accepted: 3 May 2023

Published: 4 May 2023



Copyright: © 2023 by the authors. Licensee MDPI, Basel, Switzerland. This article is an open access article distributed under the terms and conditions of the Creative Commons Attribution (CC BY) license (<https://creativecommons.org/licenses/by/4.0/>).

1. Introduction

In recent years, there has been a sharp increase in interest in electric mobility operations. Electric vehicles (EVs) are considered a crucial solution to the long-term objective of becoming carbon neutral by 2050. However, the biggest obstacle to recent EV breakthroughs is still energy storage. Due to their long lifespan and high energy density, rechargeable lithium-ion batteries are utilized in most EVs all over the world. Unfortunately, a battery of this type is vulnerable to mechanical, electrical, and thermal stresses [1–3]. Vibrations from rough road surfaces or shocks during collisions are typical causes of mechanical abuse in vehicles. Meanwhile, conventional vehicles and EVs use various complex electronics to operate, such as gauges, lights, ignition systems or inverters, and air conditioning systems. Many electric circuits and wiring need to be well conditioned to prevent short circuits. Lastly, thermal abuse in a vehicle may appear in the form of overheating, particularly in energy storage systems, which can be caused by extreme atmospheres and overcharging, overload discharge, or internal electro-chemical failures. Any abuse of the battery cell may cause a performance decrease or even a hazardous thermal runaway when uncontained [4–6]. To prevent this, an ample thermal management system needs to be established.

Current Li-ion batteries used in EVs have a typical optimum temperature range between 25 and 40 °C, which balances their performance and life cycle [7–9]. To pre-

vent overheating and subsequent thermal runaway, various thermal protection methods have been developed and reported in recent years, such as liquid or air cooling [10,11], phase-change materials [12–15], heat pipes [16–18], and hybrid cooling methods [19–21]. Although extensive research has been conducted, major obstacles remain in terms of vehicle performance, cost, and safety issues.

Phase-change materials (PCMs) are known for their superior latent heat capacity, that is, they act as heat absorbers without notable temperature increases. PCMs can be used in many modern engineering applications, such as automotives [22–24], photovoltaics [25–27], and buildings [28–31], due to their simplicity and affordability on the market. PCMs can provide passive thermal protection, necessitating no additional power supply. Additionally, PCMs can release trapped heat into their surroundings when no heat is transferred internally, making them reversible heat absorbers. PCMs are also considered superior for maintaining thermal uniformity between battery cells [32]. However, organic materials with relatively poor thermal conductivity make up the majority of PCMs within the optimum temperature range for Li-ion batteries, which therefore limits their effectiveness. Despite this, paraffin and fatty acids are often used due to their relatively constant thermal and chemical characteristics, resilience to corrosives, and affordability compared to inorganic materials. Both are currently considered promising materials for battery thermal management applications because of these characteristics, and comparisons with other PCM types have been thoroughly reviewed, such as in [24]. Several additions, including graphite/graphene, metal compounds, and nanoparticles, could be used to improve the issue of thermal conductivity [27,33]. However, there are still several other limitations, such as weight and environmental side effects, while metal additives in particular require additional protection against corrosion.

Adding PCM to the EV battery module or pack comes with its own challenges. The use of porous materials such as metal foams to store the PCM has been extensively studied [34–37]; however, the main challenges often concern complicated PCM insertion methods and volumetric change during phase change. Another possibility is to submerge the battery module or pack in a tight container filled with a PCM. Although this design likely produces a greater temperature uniformity, the wiring complexity and huge addition of weight are the main drawbacks. Alternatively, the PCM could be directly immersed in a certain type of textile, where fiber could also act as a material reinforcement of the composite [38]. Unfortunately, this configuration creates a relatively long distance between the heat source and the heat-absorbing material, which is undesirable at a higher discharge rate [39]. This is similar to placing the PCM in a separate carbon container [14], despite its cost-efficient and simple design, leaving an air gap between the battery and PCM that requires preventable convective heat transfer, hence delaying rapid heat absorption. A macro- or microencapsulation alternative has been proposed multiple times, despite its high manufacturing cost, low thermal conductivity, and dubious capsule strength for enduring numerous volumetric changes [40–44].

An integrated PCM composite used as a battery holder in the module was experimentally tested under varied discharge conditions and is reported in this paper. Paraffin wax and Caprylone were selected due to their different latent profiles and compared based on maximum temperature and uniformity. An organic PCM mixing into a resin composite could provide closer contact with the battery cell that dissipates heat; hence, it acts as local thermal protection, where the PCM can effectively isolate the heat dissipation between neighboring battery cells or modules. It is worth noting that any material addition needs to be carefully measured, as it reduces the EV's miles-to-weight ratio [45–47]. As such, this suggested design could provide a lightweight composite that is more economically feasible, rather than the other PCM storage types described above. A tensile test was also performed to quantify the material strength required for vehicle applications and determine whether a supplementary mechanical reinforcement was needed. Furthermore, the module composite also needs to be electrically safe to prevent short circuits, especially considering its naturally compact design. Finally, by analyzing the maximum temperature

and the degree of temperature uniformity across all the battery cells, the effectiveness and suitability of a PCM as a thermal protective layer between each cell locally and the entire battery module can be evaluated.

2. Materials and Methods

The battery module utilized in this experiment is made up of nine parallel-arranged (1S9P) 21700 lithium-ion battery cells. Table 1 lists the general specifications of this cell. All the cells are spot-welded to nickel strips and copper wires to form a single-positive and a single-negative module tab for charging and discharging processes. The experimental setup and photos are shown in Figure 1. The module case was made using MEKP (Methyl Ethyl Ketone Peroxide) and Ripoxy R-804 Vinyl Ester Resin purchased from Justus Kimiaraya, Indonesia. Two comparable battery module cases were also manufactured, each with 20% wt Paraffin-20 mix or Caprylone PCM. A higher PCM amount was used but to no avail as the PCM became no longer fully enclosed by the resin, and thus failed the repeated cycle test due to the PCM leak. These analytical grade organic PCMs were purchased from Sigma-Aldrich Singapore. Both PCM samples had their melting points and latent heat capacities measured using the NETZSCH DSC214 Polyma Differential Scanning Calorimetry (DSC) (Germany) in N₂ atmosphere. Then, 5% wt graphite (G) powder was added to the composite mixture to enhance its overall conductive heat transfer. All of these materials were heated in a water bath at 60 °C until all the PCM melted, slowly stirred at approximately 60 rpm for two minutes, and then poured into a 74 mm × 74 mm rectangular mold specifically designed to contain nine 21700 battery cells in a 3 × 3 configuration, with the smallest distance between cylindrical cells being 2 mm. The composite was then cured for at least 24 h before its removal from the mold, resulting in a solid battery holder, as depicted in Figure 1c. The contact part with the battery was smoothed with sandpaper before an Arctic MX4 thermal paste (less than 1 g for each module) was thinly applied on its surface to ensure maximum contact and heat dissipation possible from the battery cells to the module. The total weight of each battery module composite is 75 ± 2 g. Two separate specimens with the same composition, with and without carbon fiber as a reinforcement material, were fabricated and cut using CNC milling following the ASTM D638 and ASTM D3039 standards, respectively, in order to evaluate their mechanical properties by means of the Tinius Olsen 300SL Universal Testing Machine (UTM) (USA). The ASTM D638 is commonly utilized for material that has a plastic-like consistency. On the other hand, the ASTM D3039 was applied to the reinforced composite with high-modulus fibers, such as carbon fiber. Meanwhile, a vacuum infusion method was used for the fabrication process of the reinforced composite, where a compressor was utilized to let the liquid resin mixture slowly permeate into the fiber placed in a sealed bag. The vacuum conditions ensured that minimal air bubbles were trapped inside the composite, resulting in a more homogeneous composite.

Table 1. Specifications of the 21700 battery cell.

Parameter	Value
Rated capacity	4800 mAh
Nominal voltage	3.7 V
Max. charge voltage	4.2 V
Discharge cut-off voltage	2.75 V
Dimensions	21.2 ± 0.3 mm (diameter), 70.3 ± 0.5 mm (height)
Mass	0.07 kg
Discharge temperature range	−20–60 °C
Expected cycle life	500 cycles > 80%

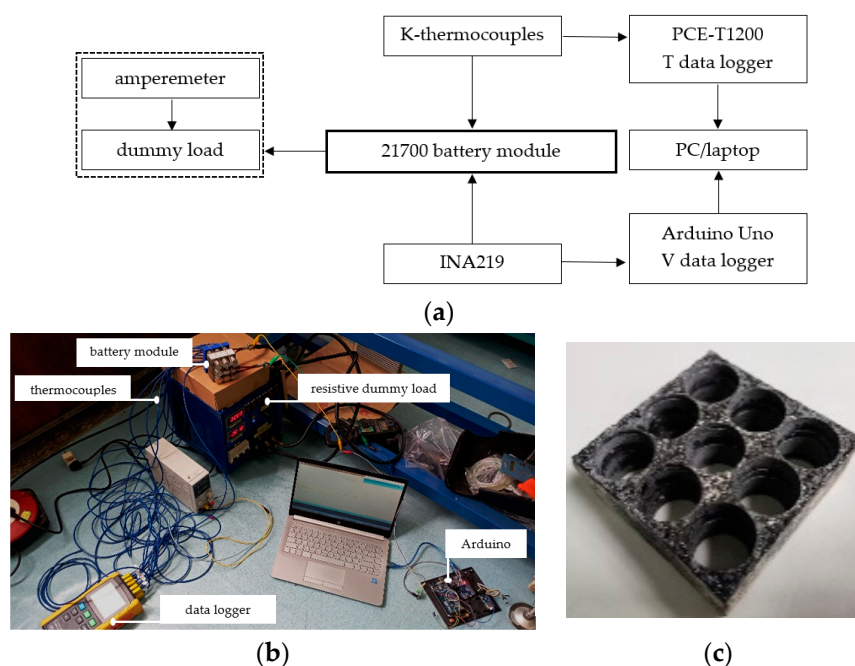


Figure 1. (a) Schematic diagram; (b) still photograph of the experimental setup, consisting of a battery module on top of a resistive dummy load connected to the data loggers; and (c) photograph of the PCM composite prepared for the 21700 battery cells.

The battery module was connected to a manually adjustable resistive dummy load. In this study, constant discharge currents of 43.2 A, 86.4 A, and 172.8 A were used, equating to discharge rates of 1 C, 2 C, and 4 C, respectively. Each battery cell had a K-type thermocouple with a standard error limit of $\pm(0.4\% + 0.5\text{ }^{\circ}\text{C})$ and a PCE-T1200 temperature data logger attached to the positive side of the cell, where typically the highest temperature can be found [14,48]. An Arduino Uno was connected to an INA219 sensor ($\pm 1\%$ accuracy) on the module terminal to record the battery module voltage throughout the run. An ambient temperature between 24 and 26 $^{\circ}\text{C}$ was maintained, and the battery module was fully charged (CC-CV) to 4.16–4.20 V prior to each run. A cut-off cell temperature and voltage of 75 $^{\circ}\text{C}$ and 2.5 V, respectively, were also implemented as safety measures. For the requirements of statistical repeatability, each experimental set was performed at least twice. In the event that an anomaly of temperature increase was found, the entire run was stopped and the respective battery cell was assessed. If defects were found from the cell inspection, the battery was replaced with a brand new one. On the other hand, if a problem with the connectors (nickel strips or cables) was found, the battery cell remained in use and the experimental measurement was restarted after the connectors were repaired. Furthermore, when the module composite was changed, a new set of battery cells was also used to nullify the potential adverse effects of cyclic aging. Finally, in addition to a visual inspection, the composite was also weighed at the end of the run. If any PCM leak was found, the measured data were discarded since the overall heat-absorbing capacity had already been affected.

3. Results and Discussion

Based on DSC measurements, the latent heat profiles of each used PCM are presented in Figure 2. Due to the possible mixture of different carbon chains, paraffin tends to have a wide melting spectrum. The overall measured latent heat capacity is 212.8 J/g, with at least two major peaks at 34.9 $^{\circ}\text{C}$ and 53.8 $^{\circ}\text{C}$. The Caprylone sample, on the other hand, displays a distinct latent heat profile with a peak at 39.4 $^{\circ}\text{C}$ and an overall latent capacity of about 277 J/g. The different latent heat characteristics of both PCMs lead to a different response toward heat dissipation [49]. The wide profile of the paraffin-filled module results

in consistent heat absorption at a slow discharge rate. As soon as the battery module reaches approximately 30 °C, heat absorption starts. On the other hand, the effective heat absorption process does not begin until as high as 36 °C in a module containing Caprylone.

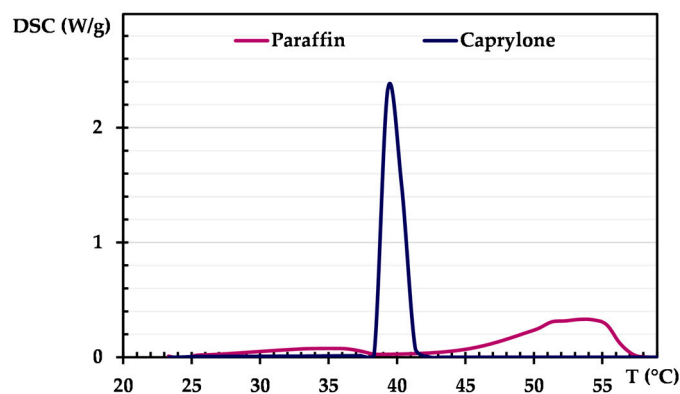


Figure 2. DSC curves for both paraffin and Caprylone samples.

The mechanical properties of the composite are typically compromised by the inclusion of paraffin. As shown in Table 2, the paraffin specimen's overall durability to resist mechanical stresses is nearly 70% lower than the composite without PCM. Graphite has the benefit of creating a more evenly distributed mixture and improving overall heat transfer, but it also further reduces the maximum force and stress. Meanwhile, PCM addition has almost no effect in terms of elongation. A dedicated battery protection system or a reinforced composite, such as carbon fiber, could address this shortcoming of EV battery pack application [50–52]. Figure 3 illustrates the substantial rise in the specimen's maximum force and stress when a carbon-fiber-reinforced PCM composite is created using the vacuum infusion process. Unfortunately, it is still challenging to fabricate a reinforced PCM composite battery module, i.e., to properly fit the carbon fiber in between the battery cells. Further developments to investigate the module strength under other direct mechanical abuses, such as object penetration and long-term vibrations, as well as a vehicle crashes, are ongoing. As such, the following thermal performance discussion in this manuscript is limited to a composite without any reinforcement materials.

Table 2. Tensile test results of the PCM composite.

Parameter	No PCM	Paraffin	Paraffin + Graphite
Ultimate force (N)	604 ± 16	225 ± 16	140 ± 35
Ultimate stress (MPa)	62.2 ± 0.9	23.2 ± 3.8	10.1 ± 2.5
Modulus (MPa)	1835 ± 135	598 ± 101	349 ± 36
Total elongation (%)	3.56 ± 0.02	3.75 ± 0.54	3.63 ± 0.21

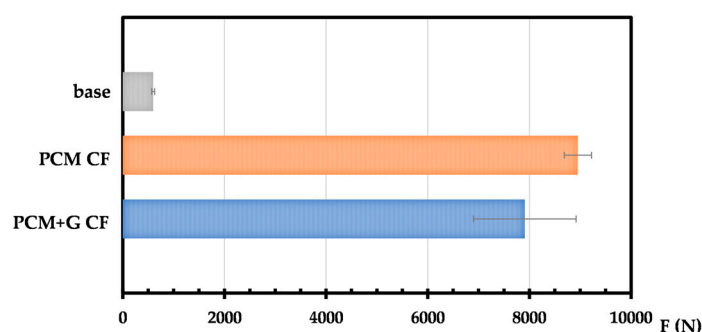


Figure 3. Effects of carbon fiber (CF) reinforcement on the maximum force.

To design and investigate the most suitable thermal management for a battery module, it is important to start from the energy balance and heat dissipation mechanism. Theoretically, the heat generation of a battery cell q can be defined as follows [1]:

$$q = q_{ir} + q_{rv} + q_s + q_m \quad (1)$$

where q_{ir} and q_{rv} are irreversible (Ohmic and polarization, including overpotential) and reversible (due to entropy change) heat generation [47,48,53], described as

$$q_{ir} = I(U - V) = I^2R \quad (2)$$

$$q_{rv} = -I \left(T \frac{\partial U}{\partial T} \right) \quad (3)$$

where U and V are the open-circuit voltage and battery operating voltage, respectively. Meanwhile, q_s is the heat generated from any side reactions, and q_m is the heat generated by mixing processes. These two terms can be neglected as long as the battery is of a good quality and does not experience serious degradation under constant current testing [1,54]. Therefore, the simplified governing equation is

$$q = q_{ir} + q_{rv} = I^2R - I \left(T \frac{\partial U}{\partial T} \right) \quad (4)$$

where I is the battery current during charge or discharge, R stands for the total internal battery resistance, and $\left(T \frac{\partial U}{\partial T} \right)$ is an entropy heat coefficient, which is affected by the battery surface temperature and state of charge (SOC). The second term sign is substituted for charge and discharge, always resulting in an exothermic process [55]. This could also explain why more heat is dissipated from the battery when the surface temperature is higher.

Figure 4 shows the typical temperature profiles and voltage depletion over time in a module casing made of pure resin, which can be used as a reference for further analysis. The so-called one C-rate corresponds to the discharge current such that a fully charged battery voltage reaches its cut-off in one hour, whereas 4 C indicates that the battery will be completely discharged in about 15 min. Considering that the heat dissipation is proportional to the square of the discharge currents (Equation (4)), it can be seen that for 1 C, 2 C, and 4 C discharge rates, the average cathode temperatures might increase to 38 °C, 50 °C, and 71 °C, respectively. Overall, there was no notable variation in temperature between the center cell temperature and the average temperature, which suggests that heat dissipation was very uniform during the discharge operation.

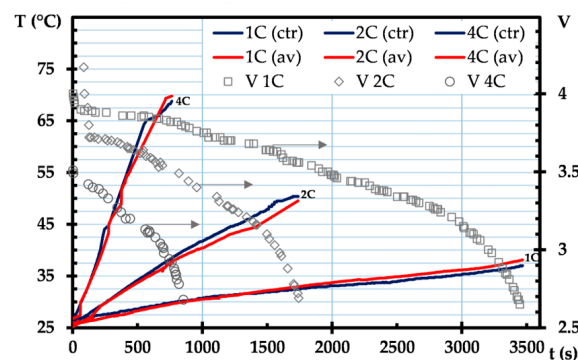


Figure 4. Average temperature (red), temperature at the center (blue), and voltage (grey) from a reference battery module without PCM under various discharge rates.

Thermal protection is provided by PCM when it is added to the battery module case matrix, reducing the impact of a battery cell's heat dissipation on its neighboring cells. As seen in Figures 5 and 6, the average temperature is notably lower than the ordinary battery module. This is due to the equally distributed PCM's ability to sufficiently absorb the heat that each cell generates. The end temperature indicates that both PCMs could protect the overall temperature at continual discharge rates up to 2 C. When the module is run at a higher discharge load, where the Li-ion battery cell normally releases more heat, as expressed in Equation (4), the temperature reduction effect is more noticeable. As for the most extreme case in this study, an additional thermal management system, such as air or liquid cooling, is vital. Additionally, since there was at least ten hours between the charging and discharging periods, and the module was kept open for natural convection, it was anticipated that the PCM would entirely release the absorbed heat, making the process reversible.

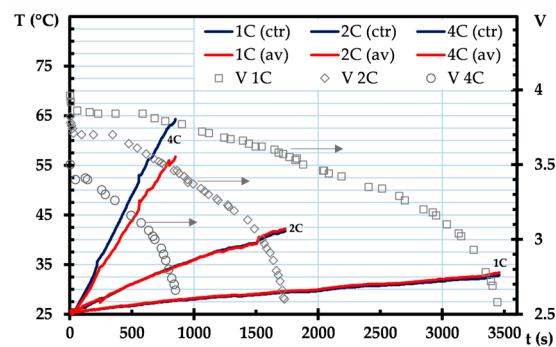


Figure 5. Average temperature (red), temperature at the center (blue), and voltage (grey) from a battery module with a paraffin composite under various discharge rates.

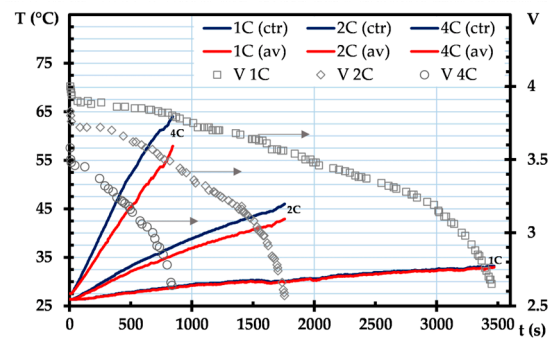


Figure 6. Average temperature (red), temperature at the center (blue), and voltage (grey) from a battery module with a Caprylone composite under various discharge rates.

There is also a notable difference between the average and middle cell temperatures for both PCMs. While there is essentially no temperature difference for lower discharge rates in the paraffin-filled case, there is a difference of more than 7 °C at the 4 C discharge rate. In contrast, in the Caprylone PCM case, even at a 2 C discharge rate, the middle temperature is already slightly higher than the overall temperature. At the end of an experiment using a 4 C discharge rate, the average temperatures are approximately 56.7 °C and 57.9 °C for paraffin and Caprylone, respectively. This could be due to the different characteristics and latent capacities of the materials, as shown earlier by DSC results. A wide latent heat profile of paraffin enables the dissipated heat to be steadily absorbed over time, successfully avoiding local heat accumulation. Furthermore, it can be seen that the deviation between the center and the mean temperatures tends to rise dramatically after the respective PCM reaches its melting peak, which occurs at 34.9 °C and 53.8 °C for paraffin and at 39.4 °C for Caprylone.

Figure 7 shows that the use of a PCM composite under a 1 C discharge rate in this study improves the overall temperature uniformity, which can be described by first using the following equation:

$$X_n = \frac{X - X_{min}}{X_{max} - X_{min}} \quad (5)$$

where X_n is the normalized value of temperature or voltage at any given time. A typical discharge process would begin ($t = 0$) with the minimum temperature T_{min} and maximum voltage V_{max} . At the end of the discharge ($t = 1$), the module voltage reaches its lowest V_{min} , and at least one of the thermocouple readings will show the maximum temperature T_{max} . The degree of uniformity is then defined as the T_n value at the end of the run since throughout the process the temperature is always expected to never decrease below the initial temperature T_{min} .

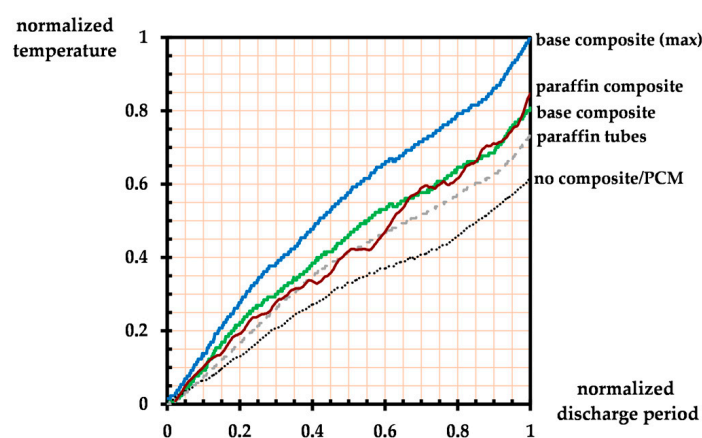


Figure 7. Temperature uniformity profile of PCM composites throughout the 1 C discharge.

A previous report shows that the degree of uniformity ranges between 0.60 and 0.79 for a battery module without any PCM and module with PCM stored in a battery-like container [14]. The uniformity range value increased to 0.88 due to the integration of PCM into the composite, which eliminated any convective heat transfer between the battery surface and PCM, allowing the dissipated heat to be locally contained. Unfortunately, the degree of uniformity for PCM composites at higher discharge rates of 2 and 4 C is substantially lower than the reference composite without PCM, as shown in Figures 8 and 9, respectively. For the paraffin composite, the discharge rates are inversely proportional to the temperature uniformity: from 0.88 at 1 C to 0.78 and 0.69 at 2 C and 4 C discharge rates, respectively. This is when the PCM heat absorbing rate can no longer cope with the dissipation rate from the cells, resulting in a larger margin between the highest and the lowest temperatures. On the other hand, the Caprylone composite shows an increasing trend, with approximately 0.68 for 2 C and 0.72 for 4 C discharge rates. Further investigations are required to depict and evaluate the PCM distribution inside the composite. Since the highest temperature typically occurs in the middle of the module, assuming that all battery cells operate in a similar condition and generate the same amount of heat. This number could be improved further if the PCM becomes somewhat more concentrated near the center rather than evenly distributed in the composite. Since the Caprylone composite seems to have a better temperature uniformity than paraffin for the 4 C discharge rate, it can be concluded that the higher latent heat capacity plays a more significant role in such a case, rather than having a wider melting temperature profile. This result is in good agreement with the previously reported comparative analysis between paraffin and fatty acid PCM [49]. Overall, the PCM composite could offer relatively adequate battery module thermal protection for at least up to a 2 C discharge rate. Given the present cost of EVs, which is greatly influenced by battery cost, as well as the necessity for effective battery recycling and waste management [56], the results from this study could support a longer life cycle of the used lithium battery, which is

advantageous. Additionally, the usage of organic PCM composite in this study could lessen its environmental impacts since recycling and reusing such materials are relatively viable.

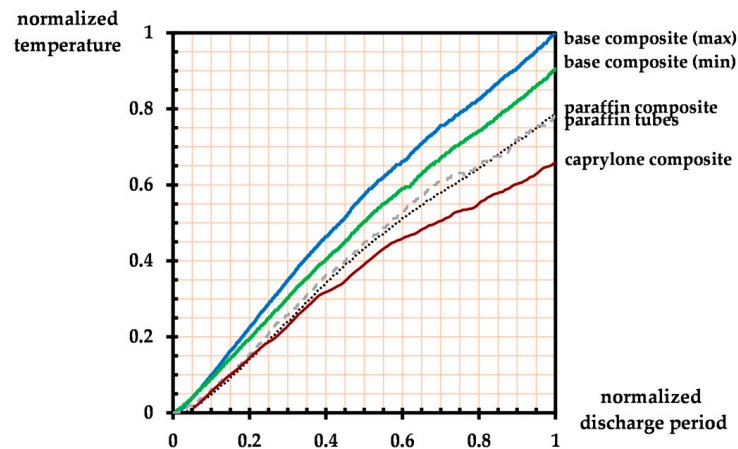


Figure 8. Temperature uniformity profile of PCM composites under 2 C discharge rate.

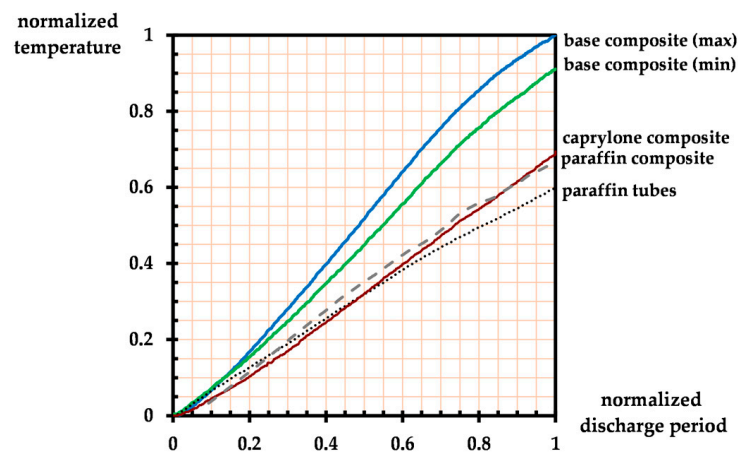


Figure 9. Temperature uniformity profile of PCM composites under 4 C discharge rate.

4. Conclusions

In this study, an experimental observation was conducted for the thermal protection against heat dissipation provided by phase-change materials (PCM) added to battery module composites. A substantially lower surface temperature might be achieved via the use of paraffin or Caprylone, whose melting temperatures are close to the temperature at which lithium-ion batteries operate at their best. However, the addition of such materials significantly reduces the overall mechanical stress of the composite by more than 50 percent. Although the use of reinforcement materials such as carbon fiber is highly encouraged to overcome this drawback, composite fabrication has become significantly more complex. Finally, it can be stated that each PCM's latent heat properties have an impact on how well they absorb heat. The use of PCM composites is proven to be better than having a separate container, especially in terms of temperature uniformity, as it has direct contact with the battery surface. Caprylone composites appear to have a better temperature uniformity than paraffin for the 4 C discharge rate, which may suggest that the higher latent heat plays a more significant role in a high C-rate condition than having a wider melting temperature profile. Nonetheless, the promising usage of both PCM as thermal protection in the EV battery module has been demonstrated, particularly for a constant discharge rate up to 2 C, where the overall temperature could be kept below 45 °C.

Author Contributions: Conceptualization, A.C.B., S., S.K. and A.H.; methodology, S. and A.C.B.; validation, S.K.; resources, M.A.P.P., A., R.R. and A.M.; experimental setup and data collection, F.S.H. and B.A.H.; writing—original draft preparation, S. and A.C.B.; writing—review and editing, B.A. and S.K.; supervision, A.M. and A.H.; funding acquisition, A.C.B. and B.A. All authors have read and agreed to the published version of the manuscript.

Funding: This study was supported in part by the Research Organization for Electronics and Informatics, BRIN under grant 2/III.6/HK/2023 and in part by the European Commission H2020 TWINNING Networking for Excellence in Electric Mobility Operations (NEEMO) Project under Grant 857484.

Data Availability Statement: The data presented in this study are available here: <https://hdl.handle.net/20.500.12690/RIN/4SF3YU>.

Acknowledgments: The authors would like to thank the Advanced Characterization Laboratories, E-Layanan Sains BRIN for the supervision platform and technical support.

Conflicts of Interest: The authors declare no conflict of interest. The funders had no role in the design of the study; in the collection, analyses, or interpretation of data; in the writing of the manuscript; or in the decision to publish the results.

References

1. Jiang, Z.Y.; Li, H.B.; Qu, Z.G.; Zhang, J.F. Recent Progress in Lithium-Ion Battery Thermal Management for a Wide Range of Temperature and Abuse Conditions. *Int. J. Hydrogen Energy* **2022**, *47*, 9428–9459. [[CrossRef](#)]
2. Feng, X.; Ouyang, M.; Liu, X.; Lu, L.; Xia, Y.; He, X. Thermal Runaway Mechanism of Lithium Ion Battery for Electric Vehicles: A Review. *Energy Storage Mater.* **2018**, *10*, 246–267. [[CrossRef](#)]
3. Kaleg, S.; Budiman, A.C.; Hapid, A.; Amin; Muharam, A.; Sudirja; Ariawan, D.; Diharjo, K. Evaluations of Aluminum Tri-Hydroxide and Pristine Montmorillonite in Glass Fiber Reinforced Polymer for Vehicle Components. *Int. J. Automot. Mech. Eng.* **2022**, *19*, 9379–9390. [[CrossRef](#)]
4. Zhao, G.; Wang, X.; Negnevitsky, M. Connecting Battery Technologies for Electric Vehicles from Battery Materials to Management. *iScience* **2022**, *25*, 103744. [[CrossRef](#)]
5. Börger, A.; Mertens, J.; Wenzl, H. Thermal Runaway and Thermal Runaway Propagation in Batteries: What Do We Talk About? *J. Energy Storage* **2019**, *24*, 100649. [[CrossRef](#)]
6. Shan, T.; Wang, Z.; Zhu, X.; Wang, H.; Zhou, Y.; Wang, Y.; Zhang, J.; Sun, Z. Explosion Behavior Investigation and Safety Assessment of Large-Format Lithium-Ion Pouch Cells. *J. Energy Chem.* **2022**, *72*, 241–257. [[CrossRef](#)]
7. Behi, H.; Karimi, D.; Behi, M.; Jaguemont, J.; Ghanbarpour, M.; Behnia, M.; Berecibar, M.; Van Mierlo, J. Thermal Management Analysis Using Heat Pipe in the High Current Discharging of Lithium-Ion Battery in Electric Vehicles. *J. Energy Storage* **2020**, *32*, 101893. [[CrossRef](#)]
8. Zhi, M.; Fan, R.; Yang, X.; Zheng, L.; Yue, S.; Liu, Q.; He, Y. Recent Research Progress on Phase Change Materials for Thermal Management of Lithium-Ion Batteries. *J. Energy Storage* **2022**, *45*, 103694. [[CrossRef](#)]
9. Budiman, A.C.; Hasheminejad, S.M.; Sudirja, S.; Mitayani, A.; Winoto, S.H. Visualization of Induced Counter-Rotating Vortices for Electric Vehicles Battery Module Thermal Management. *Front. Heat Mass Transf.* **2022**, *19*, 1–6. [[CrossRef](#)]
10. Jarrett, A.; Kim, I.Y. Design Optimization of Electric Vehicle Battery Cooling Plates for Thermal Performance. *J. Power Sources* **2011**, *196*, 10359–10368. [[CrossRef](#)]
11. Wu, W.; Wang, S.; Wu, W.; Chen, K.; Hong, S.; Lai, Y. A Critical Review of Battery Thermal Performance and Liquid Based Battery Thermal Management. *Energy Convers. Manag.* **2019**, *182*, 262–281. [[CrossRef](#)]
12. Ianniciello, L.; Biwolé, P.H.; Achard, P. Electric Vehicles Batteries Thermal Management Systems Employing Phase Change Materials. *J. Power Sources* **2018**, *378*, 383–403. [[CrossRef](#)]
13. Liu, C.; Xu, D.; Weng, J.; Zhou, S.; Li, W.; Wan, Y.; Jiang, S.; Zhou, D.; Wang, J.; Huang, Q. Phase Change Materials Application in Battery Thermal Management System: A Review. *Materials* **2020**, *13*, 4622. [[CrossRef](#)] [[PubMed](#)]
14. Budiman, A.C.; Kaleg, S.; Sudirja; Amin; Hapid, A. Passive Thermal Management of Battery Module Using Paraffin-Filled Tubes: An Experimental Investigation. *Eng. Sci. Technol. Int. J.* **2022**, *29*, 101031. [[CrossRef](#)]
15. Talluri, T.; Kim, T.H.; Shin, K.J. Analysis of a Battery Pack with a Phase Change Material for the Extreme Temperature Conditions of an Electrical Vehicle. *Energies* **2020**, *13*, 507. [[CrossRef](#)]
16. Rao, Z.; Wang, S.; Wu, M.; Lin, Z.; Li, F. Experimental Investigation on Thermal Management of Electric Vehicle Battery with Heat Pipe. *Energy Convers. Manag.* **2013**, *65*, 92–97. [[CrossRef](#)]
17. Huang, Q.; Li, X.; Zhang, G.; Zhang, J.; He, F.; Li, Y. Experimental Investigation of the Thermal Performance of Heat Pipe Assisted Phase Change Material for Battery Thermal Management System. *Appl. Therm. Eng.* **2018**, *141*, 1092–1100. [[CrossRef](#)]
18. Wrobel, R.; Reay, D. Heat Pipe Based Thermal Management of Electrical Machines—A Feasibility Study. *Therm. Sci. Eng. Prog.* **2022**, *33*, 101366. [[CrossRef](#)]

19. Lyu, Y.; Siddique, A.R.M.; Majid, S.H.; Biglarbegian, M.; Gadsden, S.A.; Mahmud, S. Electric Vehicle Battery Thermal Management System with Thermoelectric Cooling. *Energy Rep.* **2019**, *5*, 822–827. [[CrossRef](#)]
20. Wang, X.; Liu, S.; Zhang, Y.; Lv, S.; Ni, H.; Deng, Y.; Yuan, Y. A Review of the Power Battery Thermal Management System with Different Cooling, Heating and Coupling System. *Energies* **2022**, *15*, 1963. [[CrossRef](#)]
21. Can, A.; Selimefendigil, F.; Öztop, H.F. A Review on Soft Computing and Nanofluid Applications for Battery Thermal Management. *J. Energy Storage* **2022**, *53*, 105214. [[CrossRef](#)]
22. Wrobel, R. A Technology Overview of Thermal Management of Integrated Motor Drives—Electrical Machines. *Therm. Sci. Eng. Prog.* **2022**, *29*, 101222. [[CrossRef](#)]
23. Wang, S.; Li, Y.; Li, Y.Z.; Wang, J.; Xiao, X.; Guo, W. Conception and Experimental Investigation of a Hybrid Temperature Control Method Using Phase Change Material for Permanent Magnet Synchronous Motors. *Exp. Therm. Fluid Sci.* **2017**, *81*, 9–20. [[CrossRef](#)]
24. Jaguemont, J.; Omar, N.; Van den Bossche, P.; Mierlo, J. Phase-Change Materials (PCM) for Automotive Applications: A Review. *Appl. Therm. Eng.* **2018**, *132*, 308–320. [[CrossRef](#)]
25. Xu, B.; Ordóñez, J.; Rao, Z.; Xu, X.; Shabgard, H. Innovative Applications of Advanced Solar Thermal Technologies Using Phase Change Materials. *Int. J. Photoenergy* **2018**, *2018*, 5707264. [[CrossRef](#)]
26. Abdulmunem, A.R. Passive Cooling by Utilizing the Combined PCM/Aluminum Foam Matrix to Improve Solar Panels Performance: Indoor Investigation. *Iraqi J. Mech. Mater. Eng.* **2017**, *17*, 712–723.
27. Abdulmunem, A.R.; Mohd, P.; Abdul, H.; Hussien, H.A.; Ghazali, H. A Novel Thermal Regulation Method for Photovoltaic Panels Using Porous Metals Filled with Phase Change Material and Nanoparticle Additives. *J. Energy Storage* **2021**, *39*, 102621. [[CrossRef](#)]
28. Takudzwa Muzhanje, A.; Hassan, M.A.; Hassan, H. Phase Change Material Based Thermal Energy Storage Applications for Air Conditioning: Review. *Appl. Therm. Eng.* **2022**, *214*, 118832. [[CrossRef](#)]
29. Indartono, Y.S.; Suwono, A.; Pasek, A.D.; Christantho, A. Application of Phase Change Material To Save Air Conditioning Energy in Building. *ASEAN Eng. J. Part A* **2013**, *3*, 46–53.
30. Cui, Y.; Xie, J.; Liu, J.; Wang, J.; Chen, S. A Review on Phase Change Material Application in Building. *Adv. Mech. Eng.* **2017**, *9*, 1–15. [[CrossRef](#)]
31. Zsembinszki, G.; Fernández, A.G.; Cabeza, L.F. Selection of the Appropriate Phase Change Material for Two Innovative Compact Energy Storage Systems in Residential Buildings. *Appl. Sci.* **2020**, *10*, 2116. [[CrossRef](#)]
32. Bashirpour-Bonab, H. Thermal Behavior of Lithium Batteries Used in Electric Vehicles Using Phase Change Materials. *Int. J. Energy Res.* **2020**, *44*, 12583–12591. [[CrossRef](#)]
33. Kumar, R.; Mitra, A.; Srinivas, T. Role of Nano-Additives in the Thermal Management of Lithium-Ion Batteries: A Review. *J. Energy Storage* **2022**, *48*, 104059. [[CrossRef](#)]
34. Chen, J.; Yang, D.; Jiang, J.; Ma, A.; Song, D. Research Progress of Phase Change Materials (PCMs) Embedded with Metal Foam (a Review). *Procedia Mater. Sci.* **2014**, *4*, 389–394. [[CrossRef](#)]
35. Lazzarin, R.; Noro, M.; Righetti, G.; Mancin, S. Application of Hybrid PCM Thermal Energy Storages with and without Al Foams in Solar Heating/Cooling and Ground Source Absorption Heat Pump Plant: An Energy and Economic Analysis. *Appl. Sci.* **2019**, *9*, 1007. [[CrossRef](#)]
36. Babu Sanker, S.; Baby, R. Phase Change Material Based Thermal Management of Lithium Ion Batteries: A Review on Thermal Performance of Various Thermal Conductivity Enhancers. *J. Energy Storage* **2022**, *50*, 104606. [[CrossRef](#)]
37. Mehrabi-Kermani, M.; Houshfar, E.; Ashjaee, M. A Novel Hybrid Thermal Management for Li-Ion Batteries Using Phase Change Materials Embedded in Copper Foams Combined with Forced-Air Convection. *Int. J. Therm. Sci.* **2019**, *141*, 47–61. [[CrossRef](#)]
38. Guimarães, T.C.; Gomes, O.d.F.M.; Oliveira de Araujo, O.M.; Tadeu Lopes, R.; da Gloria, M.Y.R.; Toledo Filho, R.D.; Koenders, E.; Caggiano, A.; Mankel, C.; Nazari Sam, M.; et al. PCM-Impregnated Textile-Reinforced Cementitious Composite for Thermal Energy Storage. *Textiles* **2023**, *3*, 98–114. [[CrossRef](#)]
39. Kadam, G.; Kongi, P. Battery Thermal Management System Based on PCM with Addition of Nanoparticles. *Mater. Today Proc.* **2023**, *72*, 1543–1549. [[CrossRef](#)]
40. Rathore, P.K.S.; Shukla, S.K. Potential of Macroencapsulated Pcm for Thermal Energy Storage in Buildings: A Comprehensive Review. *Constr. Build. Mater.* **2019**, *225*, 723–744. [[CrossRef](#)]
41. Kheradmand, M.; Castro-Gomes, J.; Azenha, M.; Silva, P.D.; De Aguiar, J.L.B.; Zoorob, S.E. Assessing the Feasibility of Impregnating Phase Change Materials in Lightweight Aggregate for Development of Thermal Energy Storage Systems. *Constr. Build. Mater.* **2015**, *89*, 48–59. [[CrossRef](#)]
42. Adesina, A. Use of Phase Change Materials in Concrete: Current Challenges. *Renew. Energy Environ. Sustain.* **2019**, *4*, 9. [[CrossRef](#)]
43. Wang, F.; Nasajpour-Esfahani, N.; Alizadeh, A.; Fadhil Smaism, G.; Abed, A.M.; Hadrawi, S.K.; Aminian, S.; Sabetvand, R.; Toghraie, D. Thermal Performance of a Phase Change Material (PCM) Microcapsules Containing Au Nanoparticles in a Nanochannel: A Molecular Dynamics Approach. *J. Mol. Liq.* **2023**, *373*, 121128. [[CrossRef](#)]
44. Memon, S.A.; Cui, H.; Lo, T.Y.; Li, Q. Development of Structural-Functional Integrated Concrete with Macro-Encapsulated PCM for Thermal Energy Storage. *Appl. Energy* **2015**, *150*, 245–257. [[CrossRef](#)]
45. Liu, T.; Hu, J.; Tao, C.; Zhu, X.; Wang, X. Effect of Parallel Connection on 18650-Type Lithium Ion Battery Thermal Runaway Propagation and Active Cooling Prevention with Water Mist. *Appl. Therm. Eng.* **2021**, *184*, 116291. [[CrossRef](#)]

46. Huda, N.; Kaleg, S.; Hapid, A.; Kurnia, M.R.; Budiman, A.C. The Influence of the Regenerative Braking on the Overall Energy Consumption of a Converted Electric Vehicle. *SN Appl. Sci.* **2020**, *2*, 606. [[CrossRef](#)]
47. Deng, Y.; Feng, C.; E, J.; Zhu, H.; Chen, J.; Wen, M.; Yin, H. Effects of Different Coolants and Cooling Strategies on the Cooling Performance of the Power Lithium Ion Battery System: A Review. *Appl. Therm. Eng.* **2018**, *142*, 10–29. [[CrossRef](#)]
48. Zhao, Y.; Patel, Y.; Zhang, T.; Offer, G.J. Modeling the Effects of Thermal Gradients Induced by Tab and Surface Cooling on Lithium Ion Cell Performance. *J. Electrochem. Soc.* **2018**, *165*, A3169–A3178. [[CrossRef](#)]
49. Budiman, A.C.; Kaleg, S.; Hidayat, N.A.; Silalahi, G.N.; Gani, M.N.; Sudirja; Amin; Muharam, A.; Hapid, A. Experimental Study of Two Organic Phase Change Materials in Cylindrical Containers for Battery Module Thermal Management: A Comparative Analysis. *J. Phys. Conf. Ser.* **2021**, *2047*, 012018. [[CrossRef](#)]
50. Muresanu, A.D.; Dudescu, M.C. Numerical and Experimental Evaluation of a Battery Cell under Impact Load. *Batteries* **2022**, *8*, 48. [[CrossRef](#)]
51. Arora, S.; Kapoor, A.; Shen, W. Application of Robust Design Methodology to Battery Packs for Electric Vehicles: Identification of Critical Technical Requirements for Modular Architecture. *Batteries* **2018**, *4*, 30. [[CrossRef](#)]
52. Bulla, M.; Schmandt, C.; Kolling, S.; Kisters, T.; Sahraei, E. An Experimental and Numerical Study on Charged 21700 Lithium-Ion Battery Cells under Dynamic and High Mechanical Loads. *Energies* **2023**, *16*, 211. [[CrossRef](#)]
53. Kim, K.M.; Jeong, Y.S.; Bang, I.C. Thermal Analysis of Lithium Ion Battery-Equipped Smartphone Explosions. *Eng. Sci. Technol. Int. J.* **2019**, *22*, 610–617. [[CrossRef](#)]
54. Zhao, Y.; Zou, B.; Zhang, T.; Jiang, Z.; Ding, J.; Ding, Y. A Comprehensive Review of Composite Phase Change Material Based Thermal Management System for Lithium-Ion Batteries. *Renew. Sustain. Energy Rev.* **2022**, *167*, 112667. [[CrossRef](#)]
55. Mevawalla, A.; Panchal, S.; Tran, M.K.; Fowler, M.; Fraser, R. Mathematical Heat Transfer Modeling and Experimental Validation of Lithium-Ion Battery Considering: Tab and Surface Temperature, Separator, Electrolyte Resistance, Anode-Cathode Irreversible and Reversible Heat. *Batteries* **2020**, *6*, 61. [[CrossRef](#)]
56. Sobianowska-Turek, A.; Urbańska, W.; Janicka, A.; Zawiślak, M.; Matla, J. The Necessity of Recycling of Waste Li-ion Batteries Used in Electric Vehicles as Objects Posing a Threat to Human Health and the Environment. *Recycling* **2021**, *6*, 35. [[CrossRef](#)]

Disclaimer/Publisher’s Note: The statements, opinions and data contained in all publications are solely those of the individual author(s) and contributor(s) and not of MDPI and/or the editor(s). MDPI and/or the editor(s) disclaim responsibility for any injury to people or property resulting from any ideas, methods, instructions or products referred to in the content.